Tech : Journal of Engineering Science
Vol. 2, No. 2, 2026.
e-ISSN: 3109-7790 (online)
https://jurnal.sinesia.id/index.php/tech/index

Rigour over R^2: Defensible Practice in BET Surface Area and Adsorption Kinetic Analysis

Zik Ken Ebikebina[1], Eyere Emagbetere[2], Benjamin Ufuoma Oreko[3], Chinedum Ogonna Mgbemena[4]
E-mail Korespondensi : mgbemena.ogonna@fupre.edu.ng
Federal University of Petroleum Resources, Effurun, Delta State, Nigeria.

Info Article
|Submitted: 23 July 2026 **|Revised**: 10 August 2026 **|Accepted**: 11 August 2026
|Published: 11 August 2026
How to Cite : Zik Ken Ebikebina, etc., "Rigour over R^2: Defensible Practice in BET Surface Area and Adsorption Kinetic Analysis", *Tech: Journal of Engineering Scince*, Vol. 2, No. 2, 2026, P. 236-260.

ABSTRACT

This comprehensive review synthesizes the theoretical foundations, core physical assumptions, and standardized experimental protocols required for defensible Brunauer–Emmett–Teller (BET) surface area determination and adsorption kinetic analysis. The work addresses critical methodological gaps in porous materials characterization, focusing on recurring pitfalls such as conflating mathematical goodness-of-fit (R^2) with true physical mechanism and applying fixed relative-pressure windows or linearized regressions without regard to data error structure. A systematic review and critical evaluation framework was employed, compiling authoritative guidelines, IUPAC technical recommendations, ISO 9277:2022 standards, and interlaboratory consensus studies published between 2015 and 2026. The evaluation reveals that unstandardized sample degassing protocols and arbitrary pressure-interval selections can induce discrepancies exceeding 30% in reported BET surface areas. Furthermore, algebraic linearization of non-linear kinetic frameworks (pseudo-first-order, pseudo-second-order, Elovich, and Weber–Morris intraparticle diffusion) severely distorts error distributions, resulting in biased rate constants and flawed mechanistic interpretations. To establish rigorous characterization standards, BET analysis must objectively implement Rouquerol consistency criteria, select appropriate probe gases (e.g., argon at 87 K for micropores or krypton for low-area solids), and incorporate complementary porosity techniques such as t-plot or NLDFT kernels. For kinetic modeling, non-linear regression must be prioritized alongside multi-metric statistical evaluations (such as chi-squared and residual sum of squares) corroborated by independent spectroscopic or structural evidence. The study concludes that strict adherence to standardized reporting guidelines, complete metadata disclosure, and FAIR data principles using Adsorption Information File (AIF) repositories are essential for ensuring international comparability and academic integrity, particularly when evaluating locally sourced bio-derived adsorbents and novel functional porous materials for environmental and energy applications.

Keywords: *Adsorption kinetics; BET surface area; bio-derived adsorbents; gas adsorption; IUPAC recommendations; physisorption; porous materials; reproducibility*

Introduction

Porous materials underpin many modern engineering technologies, from catalytic converters and carbon-capture systems to water-purification filters and battery electrodes. Their performance depends heavily on two interrelated properties: the total accessible surface area available for interaction with guest molecules, and the rate at which those molecules adsorb onto, or diffuse through, the material structure. As global efforts to mitigate climate change, improve industrial sustainability, and expand access to clean water accelerate, the demand for materials with precisely tailored porosity and surface reactivity has grown

rapidly across both academic research and industrial development (Chun et al., 2022; Jiang et al., 2024).

For more than eight decades, the Brunauer–Emmett–Teller (BET) gas-adsorption method has remained the IUPAC-endorsed standard for quantifying specific surface area and, in combination with complementary analyses, for characterizing pore-size distribution in porous solids (Chrouda et al., 2025; Yek et al., 2020; K. Zhang & Zhang, 2025). Even with advances in alternative techniques, including positron-annihilation lifetime spectroscopy, high-resolution electron tomography, and molecular simulation; BET analysis continues to serve as the primary benchmark for comparing materials across laboratories worldwide. Nonetheless, major collaborative studies have highlighted significant inconsistencies in how the method is applied: BET areas calculated from identical isotherms can differ substantially from one laboratory to another, and reported surface areas for nominally identical reference materials can vary by tens of percent depending on the relative-pressure range selected, the sample-pretreatment protocol, and the software settings used (Al Rammah et al., 2025; Osterrieth et al., 2022; Xia et al., 2024). These findings underscore the need for strict adherence to standardized, criterion-based procedures. Researchers have also noted that total BET surface area often correlates poorly with functional performance in real applications such as CO_2 capture or selective adsorption, where pore geometry, surface chemistry, and accessibility play decisive roles (Mgbemena et al., 2013; Odeh et al., 2025).

Alongside surface-area measurement, adsorption-kinetic modelling provides insight into the rate-limiting steps and interaction mechanisms between adsorbate and adsorbent, informing both fundamental understanding and practical process design. While the classical Lagergren pseudo-first-order, Ho–McKay pseudo-second-order, Elovich, and Weber–Morris intraparticle-diffusion models remain the most widely applied frameworks, recent reviews emphasize that statistical goodness-of-fit alone cannot establish a mechanism; complementary evidence from spectroscopy, microscopy, or isotherm analysis is essential for robust interpretation (Revellame et al., 2020; Vareda, 2023; Yazidi et al., 2026). Emerging approaches increasingly combine kinetic models with machine learning or density-functional theory to distinguish surface reaction, film diffusion, and pore diffusion, but these require well-designed datasets and transparent reporting of assumptions to yield reliable results.

These characterization tools are particularly relevant to ongoing research across sub-Saharan Africa, where locally sourced biomass, agricultural residues, and natural minerals are being developed as low-cost, sustainable adsorbents for water treatment, environmental remediation, and energy storage. Recent work has

demonstrated the potential of materials derived from baobab shells, *Canarium* and *Ricinodendron* seed husks, date pits, and chitosan–biochar composites; however, consistent and defensible adsorption characterization remains a persistent challenge, limiting international comparability and broader adoption of these promising materials (Bourafa et al., 2024; Chin et al., 2022; Ezenwa et al., 2024; C. Liu et al., 2023; Ndukwu et al., 2022; Odeh et al., 2025; Offiah & Falade, 2023).

This review synthesizes core principles, practical guidance, and critical-interpretation rules as used in peer-reviewed surface-science and materials-engineering research, drawing on authoritative guidelines and recent consensus studies from 2015 to 2026. It proceeds from fundamental theory through experimental execution, data analysis, and responsible reporting, with specific notes on what constitutes valid academic practice and, on the challenges, commonly encountered when working with novel or locally engineered materials.

Research Methods

A general review and synthesis approach was used to assess the current practices for surface area and adsorption kinetic characterization. The authors review, compile and critically evaluate the current theory, underlying assumptions and standardised procedures based on the latest results in the literature from IUPAC recommendations, interlaboratory comparisons, and peer-reviewed consensus studies, rather than create new laboratory data. The analytical framework consists of two main parts. In Part I, the Brunauer-Emmett-Teller (BET) gas-adsorption method is explored in detail, providing a discussion of basic thermodynamic concepts, pretreatment procedures, and methods of data validation, with particular emphasis on the objective methods such as the Rouquerol consistency rules and appropriate relative-pressure range selection. The adsorption kinetics are discussed in Part II, which involves the mathematical derivation, limitations of application and structure of error of various models such as pseudo-first order, pseudo-second order, Elovich, intraparticle-diffusion model. The methodology is systematic, with issues of mathematical goodness-of-fit as physical mechanism and poor linearization discussed throughout. Lastly, it gives context to these challenges to the locally sourced and bio-derived porous adsorbents to set up reproducible, internationally comparable characterization standards.

Results and discussion

Part I — BET Surface Area Analysis

2. Theoretical Background

2.1 Origins and Core Concept

The Brunauer–Emmett–Teller (BET) theory represents one of the most significant advances in surface science, first published in 1938 by Stephen Brunauer, Paul Hugh Emmett, and Edward Teller (Brunauer et al., 1938). Brunauer and Emmett developed the experimental foundation of the method at the U.S. Department of Agriculture's Fixed Nitrogen Research Laboratory in Washington, D.C., while seeking a reliable means of measuring the surface area of ammonia-synthesis catalysts; the physicist Edward Teller contributed the statistical-mechanical derivation that generalised the Langmuir treatment to multilayer adsorption. The theory was developed explicitly to address a fundamental limitation of the Langmuir adsorption model, which had dominated the description of gas–solid interactions since 1916. Langmuir's theory assumes that adsorption is limited to a single molecular layer, that every adsorption site is energetically identical, and that adsorbed molecules do not interact; conditions rarely satisfied in practice, especially on high-surface-area materials or at higher pressures (Langmuir, 1917).

The BET model extends this framework by introducing multilayer adsorption. It posits that adsorption proceeds in successive stages: the first layer of adsorbate molecules binds directly to the solid surface through van der Waals or, in some systems, chemical forces; once the first layer is partially or fully occupied, incoming molecules adsorb onto already adsorbed molecules, forming second, third, and subsequent layers. A key physical distinction is embedded in the model: the enthalpy of adsorption for the first layer differs from that of all subsequent layers, which are assumed to interact with one another with the same energy as the bulk liquefaction of the adsorbate. This assumption is consistent with the observation that physisorbed layers beyond the first behave much like a thin liquid film.

Experimentally, the method relies on measuring the volume of gas adsorbed onto a solid sample as a function of pressure at constant temperature; an adsorption isotherm. Nitrogen at its boiling point (77 K under atmospheric pressure) is the traditional standard probe gas, chosen for its chemical inertness, well-characterized molecular size, and suitable vapour-pressure range at cryogenic temperatures. It is now recognised, however, that the quadrupole moment of N_2 produces specific interactions with polar surface sites and functional groups, which can bias the orientation and packing of adsorbed molecules and hence the effective cross-sectional area. For this reason, current IUPAC guidance recommends argon at 87 K

for high-resolution micropore analysis, and krypton at 77 K for materials of very low surface area (see Sections 2.2 and 3.1).

The linear BET equation, derived by balancing the rates of adsorption and desorption for each molecular layer, is expressed as:

$$\frac{P}{V(P_0-P)} = \frac{1}{V_m C} + \frac{(C-1)}{V_m C} \times \frac{P}{P_0} \quad (1)$$

Where:

P = Equilibrium pressure of the adsorbate gas at the measurement point

P_0 = Saturation vapour pressure of the pure adsorbate at the experimental temperature

V =Total volume of gas adsorbed at Pressure P, expressed at standard temperature and pressure

V_m = Hypothetical volume of gas required to form a single, complete monolayer covering all accessible surfaces of the sample

C = Dimensionless BET constant, related exponentially to the difference between the enthalpy of adsorption of the first layer (ΔH_1) and the enthalpy of liquefaction of the bulk adsorbate (ΔH_L) such that:

$$C \propto \exp\left(\frac{\Delta H_1 - \Delta H_L}{RT}\right) \quad (2)$$

When experimental adsorption data are plotted with $\frac{P}{V(P_0-P)}$ on the vertical axis and $\frac{P}{P_0}$ on the horizontal axis, a linear relationship should emerge within a defined pressure interval. The values of V_m and C are then derived algebraically from the slope and intercept of the best-fit straight line:

$$\text{Slope} = \frac{(C-1)}{V_m C}, \text{ Intercept} = \frac{1}{V_m C}$$

From these the monolayer volume is calculated as:

$$V_m = \frac{1}{\text{Slope} + \text{Intercept}} \quad (3)$$

2.2 Main Assumptions and Limitations

The utility of the BET model rests on a set of simplifying assumptions that enable mathematical treatment but also define its boundaries of applicability. These assumptions are frequently overlooked in routine analysis, leading to flawed or misleading results:

i. **Surface energetic homogeneity.** The model treats the entire solid surface as having uniform adsorption energy, with no preferential sites or structural heterogeneity. Most materials, including zeolites, metal–organic frameworks (MOFs), biochars, and engineered catalysts, exhibit a distribution of surface energies arising from defects, edges, crystal faces, and functional groups.

ii. **Absence of lateral interactions.** Adsorbed molecules are assumed to exert no attractive or repulsive forces on one another. While reasonable at low

coverage, this breaks down at higher loadings where molecular proximity increases.

iii. **Constant enthalpy for upper layers.** All layers beyond the first are assumed to have an adsorption enthalpy identical to the heat of condensation of the bulk adsorbate. Deviations occur when pore dimensions approach the size of the adsorbate molecule, where overlapping attractive forces from opposite pore walls alter adsorption energetics.

iv. **Unrestricted multilayer formation.** The model implicitly assumes that layers can grow without bound, which is not true in confined spaces such as micropores or narrow mesopores, where pore walls are separated by only a few molecular diameters.

A robust body of interlaboratory work confirms that correct selection of the relative-pressure range is the single most critical factor in obtaining reliable BET data. For nonporous, macroporous, and many mesoporous solids, approximately linear behaviour is observed between $P/P_0 \approx 0.05$ and 0.35, and this interval is a reasonable default (Osterrieth et al., 2022; Thommes et al., 2015). It is essential to recognise, however, that this window is not universal. Below the lower bound, enhanced adsorption in micropores or on high-energy sites departs from multilayer behaviour; above the upper bound, capillary condensation in mesopores fundamentally alters the mechanism and invalidates the model. For microporous materials (Type I isotherms), the applicable BET interval typically lies at substantially lower relative pressures and must be identified using objective criteria rather than assumed. Including points outside the valid window can introduce errors in calculated surface area exceeding 30 %, even for well-characterized reference materials.

To place the choice of range on an objective footing, the Rouquerol consistency criteria should be applied when selecting the interval (Section 3.2). The BET constant C also serves as a vital diagnostic of whether the model is appropriate for the material:

i. **A negative intercept** on the BET plot indicates that the selected pressure range is invalid, or that the material's adsorption behaviour fundamentally violates the BET assumptions, commonly seen in ultra-microporous solids or materials with strong specific chemical interactions.

ii. **A very high C value (> ~150–200)** typically signals strong adsorbate–surface interactions or dominant micropore filling and calls for complementary methods, such as the t-plot, Dubinin–Radushkevich, or Horvath–Kawazoe analysis, rather than standard BET interpretation.

iii. **A very low C value (< ~20)** suggests weak surface–adsorbate interaction, often found in non-polar or highly graphitized materials, where the linear region may be narrower or less well defined.

2.3 Calculation of Specific Surface Area

Once the monolayer volume V_m has been determined from a valid linear BET plot, the specific surface area S_{BET} (in square metres per gram of solid) is calculated from fundamental physical constants and the known molecular dimensions of the adsorbate:

$$S_{BET} = \frac{V_m \times N_A \times \sigma}{m \times V_{mol}} \quad (4)$$

Where:

N_A =Avogadro's constant (6.022×10^{23} molecules mol^{-1}), representing the number of molecules in one mole of gas

σ = cross-sectional area of a single adsorbate molecule; for nitrogen at 77K, the internationally accepted value is 0.162nm^2, derived from the close-packed liquid arrangement of nitrogen molecules

m = mass of the sample analyzed, measured after complete degassing to remove all pre-adsorbed contaminants.

V_{mol} = molar volume of an ideal gas at standard temperature and pressure (22.414×10^{-3} $m^3 mol^{-1}$ or 22.414 L mol^{-1})

This calculation converts the measured gas volume into the number of molecules required to form a single layer, multiplies by the area each molecule occupies, and normalizes by sample mass to yield an intrinsic material property independent of sample size. Because adsorbed-gas volumes are conventionally reported at STP, the reference state must be applied consistently: in adsorption practice, STP denotes 273.15 K and 101.325 kPa (for which V_{mol} = 22.414 L mol^{-1}), and this convention should be stated explicitly to avoid ambiguity with the post-1982 IUPAC definition of standard pressure (100 kPa).

It is important to emphasize that the resulting value is an *apparent* surface area, derived from a simplified physical model and dependent on the probe gas and experimental conditions. It does not represent an absolute "true" surface area, nor does it account for pores smaller than the kinetic diameter of the adsorbate molecule. Values should therefore always be reported as the BET specific surface area, with clear specification of the adsorbate gas and temperature. Where microporosity is significant, the total BET area should be accompanied by separate estimates of external and micropore surface area obtained from complementary methods.

Figures 1-3 depicts the Nitrogen Adsorption-Desorption Isotherm, BET Adsorption Isotherm and the Langmuir Adsorption Plot.

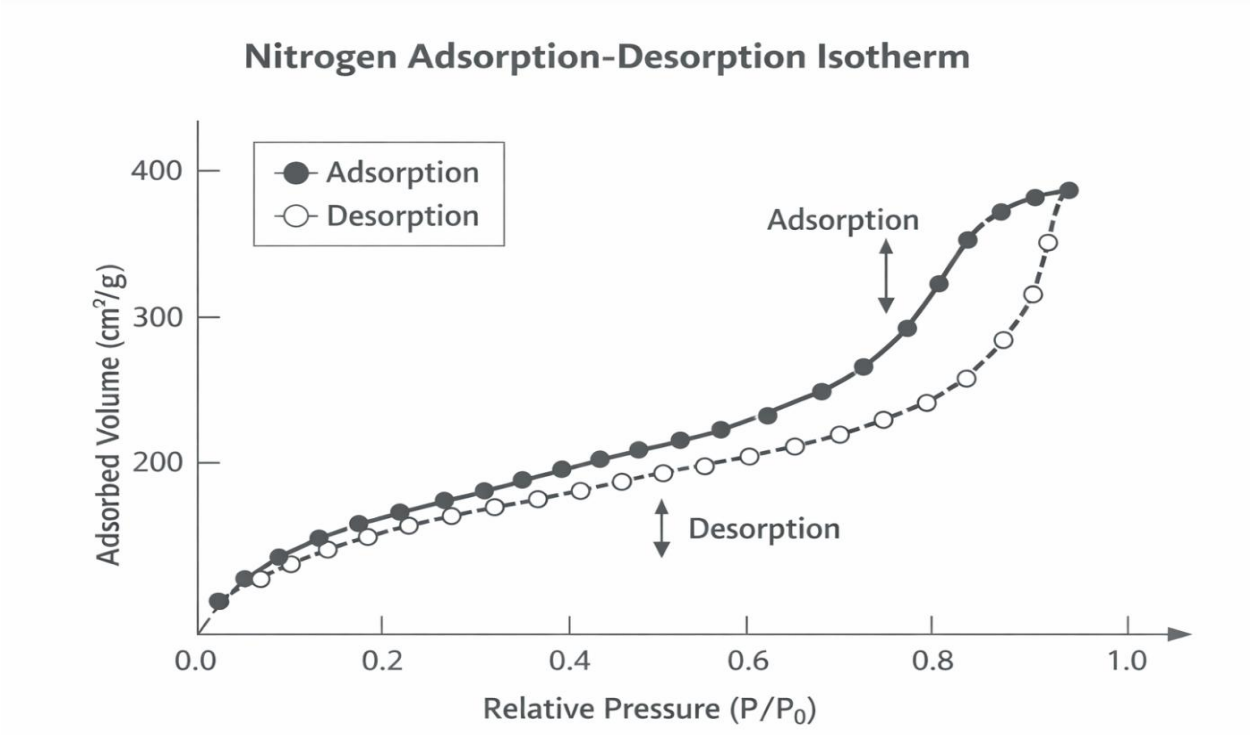

Figure 1. Nitrogen Adsorption-Desorption Isotherm

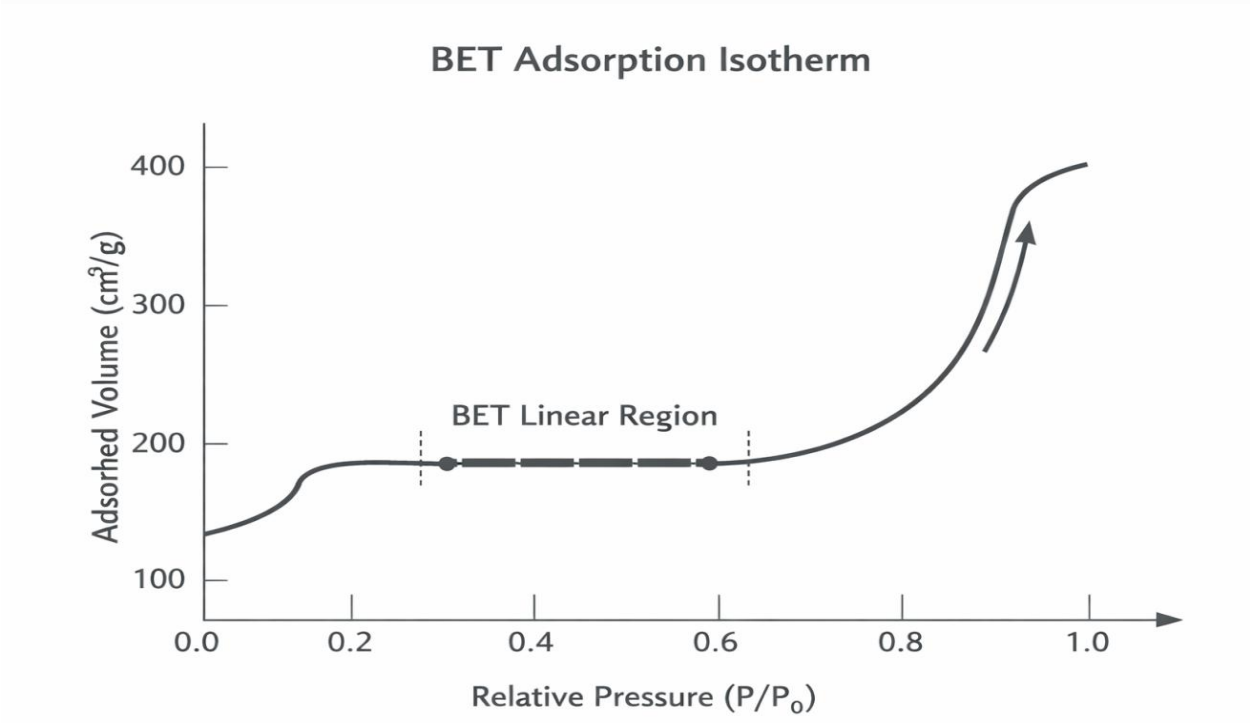

Figure 2. BET Adsorption Isotherm

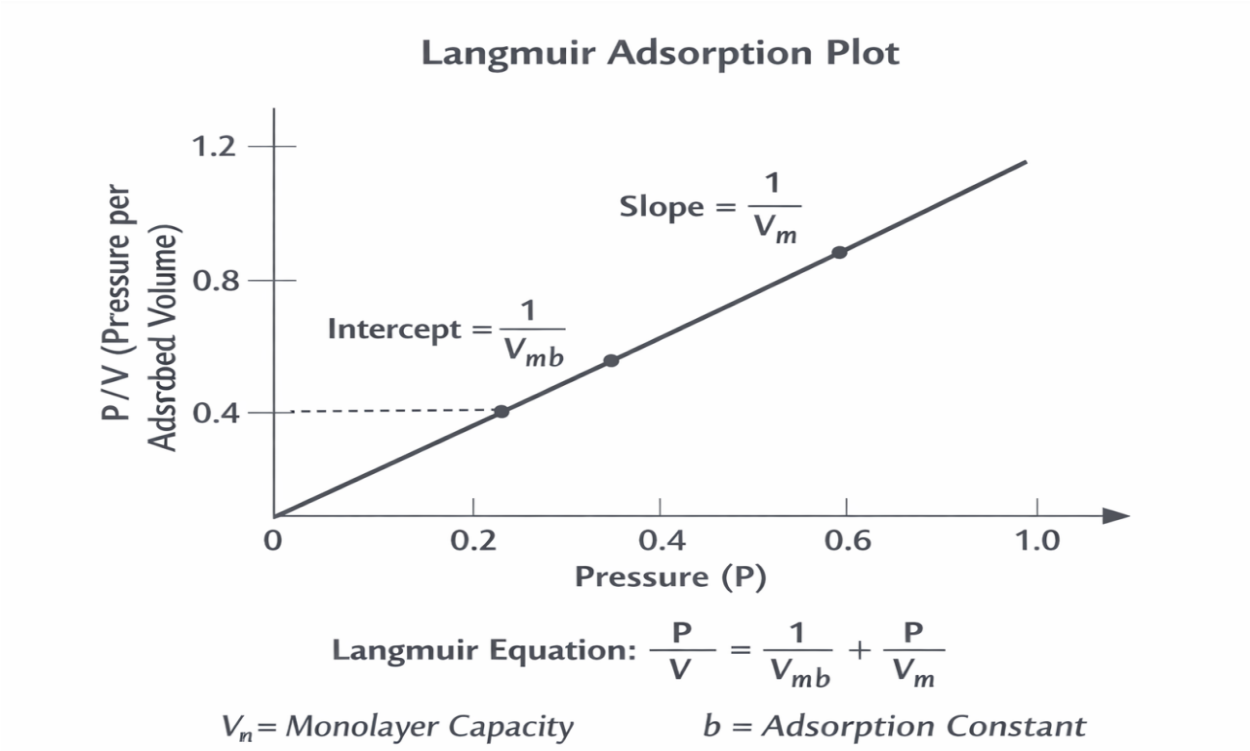

Figure 3. Langmuir Adsorption Plot

3. Experimental Procedure and Best Practices

3.1 Sample Preparation

The reliability of all subsequent BET calculations rests on rigorous sample pretreatment, widely recognised as the single greatest source of avoidable error in gas-adsorption analysis. Before measurement, samples must be thoroughly degassed to remove physisorbed moisture, atmospheric carbon dioxide, residual solvents, and volatile organic contaminants that would otherwise occupy adsorption sites, block pore entrances, or distort the measured isotherm. The objective is to restore the material's native accessible surface and pore network without altering its intrinsic structure or chemistry.

Standard practice involves heating samples under dynamic vacuum (~10^{-3}–10^{-1} Pa) or flowing high-purity inert gas (nitrogen, argon, or helium) for 4–12 hours. Temperature must be matched to material type:

i. **Metal oxides, silicas, and most carbon materials:** typically, 150–250 °C;
ii. **Zeolites, MOFs, COFs, and thermally sensitive frameworks:** 80–150 °C, validated to avoid structural collapse or ligand loss;
iii. **Polymers, bio-derived adsorbents, and organo-functionalised materials:** 50–120 °C, often under reduced pressure only.

Insufficient degassing leaves contaminants in place, yielding artificially low apparent surface area; conversely, excessive temperature or prolonged heating may cause sintering, phase transformation, or pore collapse, giving artificially high or

misleading values. Interlaboratory studies confirm that variations in degassing protocol alone can produce differences of 15–35 % in BET results for identical reference materials (Osterrieth et al., 2022).. Where material stability is uncertain, thermogravimetric analysis (TGA) is strongly recommended to establish safe pretreatment limits before adsorption measurements.

Sample mass is another critical yet frequently overlooked parameter. ISO 9277:2022 and IUPAC guidance specify that the total absolute surface area of the analysed portion should be at least ~1–20 m^2 to ensure an adequate signal-to-noise ratio and accurate pressure measurement. For materials of inherently low surface area such as dense ceramics, metals, coatings, or thin films, standard nitrogen adsorption becomes unreliable because the quantity of gas adsorbed approaches the instrument detection limit. In such cases, krypton adsorption at 77 K is preferred: its much lower saturation vapour pressure increases sensitivity, enabling reliable measurement down to ~0.05 $m^2\ g^{-1}$. This approach has proven valuable for thin films, supported catalysts, and engineered surfaces where nitrogen yields poor precision.

3.2 Measurement and Data Validation

Acquisition of a robust adsorption isotherm requires careful control of experimental conditions and adherence to established protocols. For multipoint BET analysis, the accepted standard is at least five, and preferably more, data points should be collected within the validated relative-pressure range appropriate to the material. Single-point measurements, though sometimes used for rapid screening, are discouraged in formal reporting because they cannot verify linearity and introduce systematic bias. The bath temperature must be held constant at 77 K (liquid nitrogen) or 87 K (liquid argon) throughout the run; deviations alter equilibrium pressures and invalidate the isotherm.

Once acquired, data must be validated before calculation:

1) **Linearity.** The regression coefficient (R^2) of the BET plot should be ≥ 0.995 as a minimum, with ≥ 0.999 preferred for high-confidence work. Lower values indicate poor conformity to BET assumptions or inclusion of points outside the valid range.
2) **Rouquerol consistency criteria.** The BET constant C must be positive, and the transformed quantity $V\ (P_0 - P)/P$ must increase monotonically with P/P_0 across the selected range; the monolayer point (P/P_0 corresponding to V_m) should fall within the chosen interval. These criteria, rather than a fixed window, should govern range selection, especially for microporous materials (Galarneau et al., 2018; J. Rouquerol et al., 2007).

3) **Model applicability.** A negative intercept or an unreasonably high C signals that the model is not physically appropriate, typically owing to dominant micropore filling or strong specific interactions.

Crucially, the total BET area does not distinguish external from internal pore surfaces, nor does it reveal how area is distributed across pore-size regimes. For microporous materials, activated carbons, zeolites, MOFs, and biomass-derived adsorbents, BET alone is insufficient, and supplementary methods are required:

i. **t-plot method** separates total area into external (meso-/macropore) and micropore contributions, and estimates micropore volume;
ii. **Dubinin–Radushkevich (DR) and Dubinin–Astakhov (DA) models:** provide more reliable assessment of micropore volume and characteristic adsorption energy;
iii. **NLDFT / QSDFT kernel methods:** deliver pore-size distributions across micro-, meso-, and macropore ranges, consistent with current IUPAC recommendations.

Figure 4 depicts the Adsorption Analysis methods.

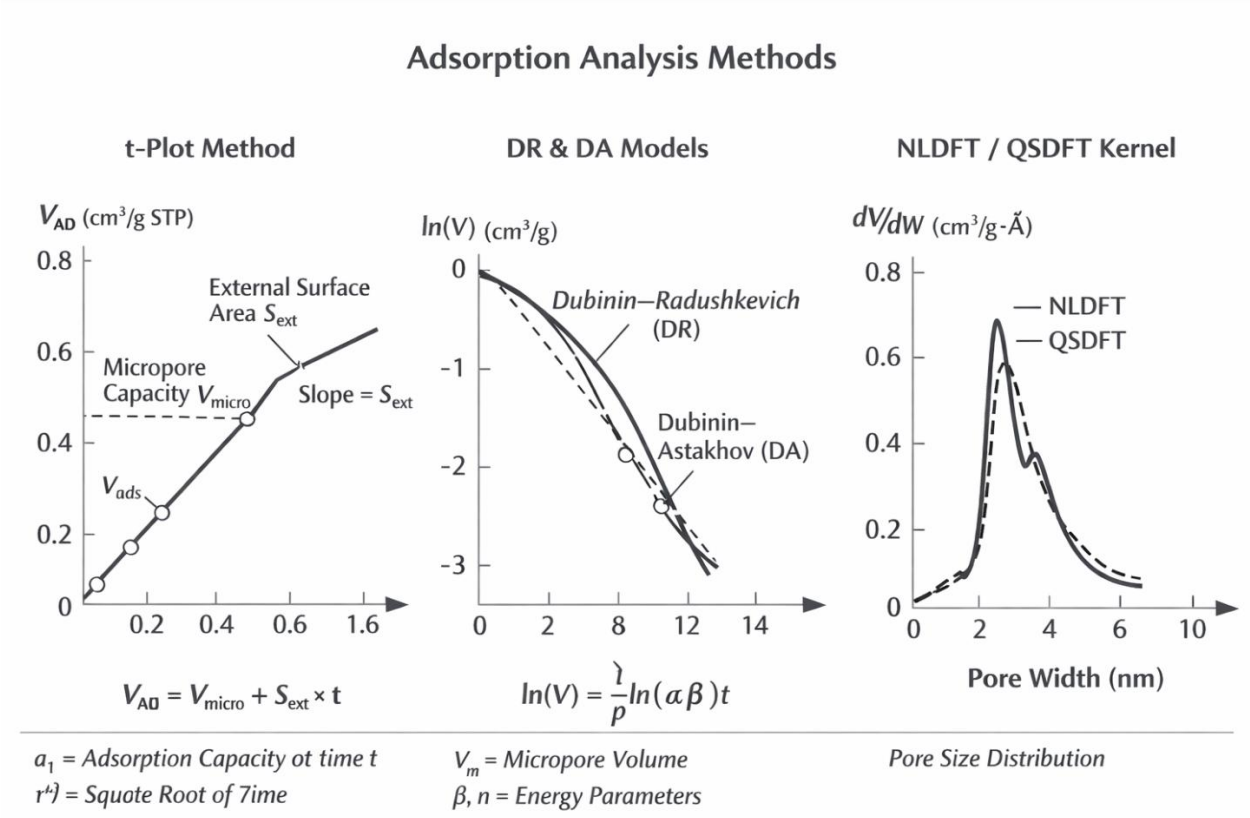

Figure 4. Depiction of t-plot, DR & DA plot and NLDFT/QSDFT Kernel plots

3.3 Reporting Standards and Common Mistakes

Transparent, complete reporting is essential for reproducibility and meaningful comparison across studies, yet surveys consistently show that a large

proportion of published work omits critical details. To meet current standards and peer-review expectations, manuscripts must state explicitly:

1) **Pretreatment conditions:** temperature, duration, atmosphere (vacuum or flowing gas), and pressure level;
2) **Adsorbate gas and experimental temperature;**
3) **Relative-pressure range:** the selected P/P_0 interval, the number of data points, and the rationale (including the criteria used) for range selection;
4) **Derived parameters:** slope, intercept, R^2, V_m, C, and calculated S_BET with units;
5) **Complementary analyses:** any t-plot, DR/DA, or NLDFT/QSDFT results used to characterise porosity.

3.4 Frequent Errors That Undermine Academic Rigour

Common mistakes identified across recent BET reproducibility and error-analysis studies include:

1) selecting pressure points arbitrarily, or adjusting the range solely to improve R^2 without physical justification;
2) using ambiguous or non-standard units (e.g. failing to specify the STP reference state for gas volumes);
3) reporting only the final surface-area value without supporting linearity diagnostics;
4) treating BET values as an "absolute" surface area rather than a model-dependent estimate tied to the probe gas;
5) ignoring the distinction between total, external, and micropore surface area, leading to misleading functional interpretations.

3.5 FAIR Data Principles and Standardised Formats

Adherence to FAIR (Findable, Accessible, Interoperable, Reusable) data principles, including depositing raw isotherm data in repositories and using standardised formats such as the Adsorption Information File (AIF), is increasingly recommended and sometimes required by journals to strengthen confidence in reported results.

Part II — Adsorption Kinetics

4. Theoretical Framework

Adsorption kinetics describes the rate at which an adsorbate transfers from the bulk fluid phase to the adsorbent surface and identifies the step or steps that limit the overall rate. Unlike adsorption thermodynamics, which establishes whether a process is energetically favourable and the maximum uptake achievable at equilibrium, kinetic analysis reveals how rapidly equilibrium is approached and

provides mechanistic insight into mass transport and surface interaction. It is essential for designing continuous-flow systems, estimating contact times, scaling up treatment processes, and interpreting adsorbent performance under dynamic conditions.

All widely used kinetic models are semi-empirical: derived from simplified physical assumptions, they are evaluated by how well they align with experimental data, but mathematical fit alone does not constitute proof of mechanism (Francis et al., 2023; Goel et al., 2021; Hameed & Ahmad, 2009; T. Liu et al., 2022; Tong et al., 2018; Wang et al., 2017). A further methodological caution applies to how these models are fitted. Most are traditionally cast in linearized form and fitted by ordinary linear regression; however, the algebraic transformations required to linearize them distort the error structure of the data and can substantially bias the estimated rate constants and equilibrium capacities. Current best practice is therefore to fit the original (non-linearized) integrated or differential forms by nonlinear regression, reserving the linear plots for illustration only, and to test several models comparatively while corroborating conclusions with independent evidence such as isotherm behaviour, surface spectroscopy, or direct visualisation of pore structure (Intriago et al., 2026; Vashishtha & Kumar, 2026).

4.1 Pseudo-First Order (Lagergren) Model

Proposed by Lagergren in 1898, this is the earliest formalised model for solid–liquid adsorption, derived by analogy to first-order chemical-reaction kinetics (Lagergren, 1898). It assumes that the rate of adsorption is proportional to the number of unoccupied adsorption sites, with the driving force being the difference between the amount adsorbed at equilibrium and the amount adsorbed at time t. The integrated linear form is:

$$\ln(q_e - q_t) = \ln q_e - k_1 t \quad (5)$$

where:

q_e = mass of adsorbate adsorbed per unit mass of adsorbent at equilibrium (mgg^{-1});

q_t = mass of adsorbate adsorbed per unit mass of adsorbent at time t (mg g^{-1});

k_1 = pseudo-first-order rate constant (min^{-1})

The model assumes a reversible process governed solely by the rate of attachment to surface sites, with no resistance from diffusion through fluid films or pore networks. It is most often applicable only over the initial 20–30 % of uptake, where surface binding is fastest and transport limitations have not yet become dominant. A good linear fit is frequently reported, but comparison of the calculated and experimental q_e often reveals substantial discrepancy; the most common diagnostic sign that the model does not describe the full adsorption process.

4.2 Pseudo-Second-Order Model

Developed to address the limitations of first-order kinetics and popularised by Ho and McKay (1999), this model assumes that the rate-limiting step involves chemical interaction between adsorbate and adsorbent, with the rate proportional to the square of the number of available surface sites (Ho & McKay, 1999). Its linearized form is:

$$\frac{t}{q_t} = \frac{1}{k_2 q_e^2} + \frac{t}{q_e} \quad (6)$$

where k_2 is the pseudo-second-order rate constant (g mg^{-1} min^{-1}).

The model implicitly incorporates assumptions of chemisorption, electron sharing or exchange, and rate dependence on the availability of reactive sites. Unlike the first-order model, it typically predicts equilibrium uptakes that closely match experiment for a wide range of adsorbate–adsorbent pairs. It is critical to emphasize, however, that a good fit does not by itself confirm chemisorption as the exclusive mechanism; physisorption on energetically heterogeneous surfaces, or combined transport–reaction control, can also yield high correlation coefficients, and the linearized form is mathematically predisposed to produce high R^2 values. Reliable interpretation requires supporting evidence such as activation-energy estimates, temperature-dependent studies, or spectroscopic identification of surface bonds. Figure 5 shows the kinetic model comparison of the Pseudo-First-Order and the Pseudo-Second-Order Model plots.

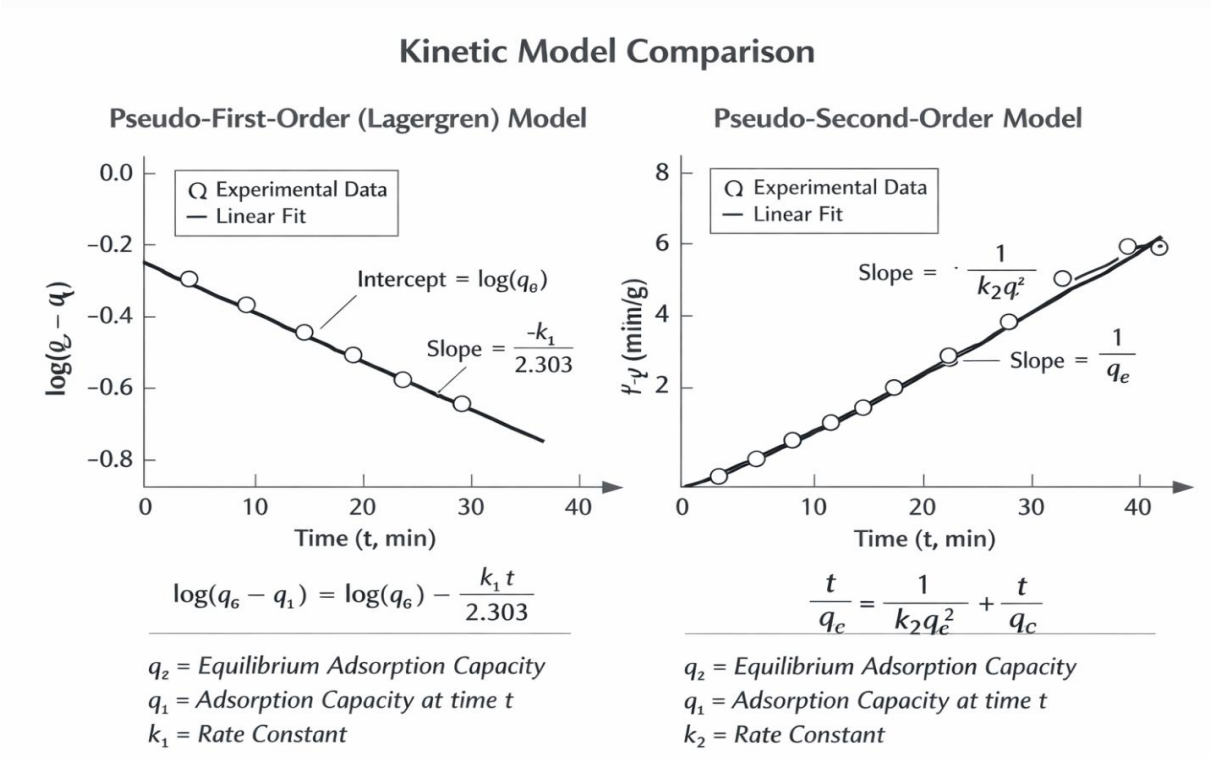

Figure 5. Pseudo-First-Order vs. Pseudo-Second-Order Model plots

4.3 Elovich Model

Originally formulated to describe gas–solid chemisorption on heterogeneous surfaces and later adapted for liquid-phase adsorption, the Elovich equation assumes that adsorption sites exhibit a continuous distribution of activation energies that increase linearly with surface coverage, so that, as sites are occupied, further adsorption requires progressively higher energy.

The Elovich equation is expressed as:

$$\frac{dq_t}{dt} = \alpha e^{-\beta q_t} \quad (7)$$

Where:

α = Initial adsorption rate (mg/gmin), β = Desorption constant related to the magnitude of the activation-energy increase with coverage (g/mg)

Integrating the equation and applying the boundary conditions yields the linear form:

$$q_t = \frac{1}{\beta}\ln(\alpha\beta) + \frac{1}{\beta}\ln t \quad (8)$$

A plot of q_t versus $\ln t$ provides β and α, which help in understanding the adsorption process.

A strong linear correlation is widely interpreted as indirect evidence that the adsorbent surface is energetically heterogeneous and that adsorption involves chemical bonding or strong specific interactions. The model is particularly useful for biomass-derived materials, layered clays, and functionalised carbons, where surface functional groups and structural defects create a broad spectrum of site energies. It is not suitable for purely physisorptive systems on highly uniform surfaces (Ganguly et al., 2020; Pap et al., 2025; Ramezanipour Penchah et al., 2022). Figure 6 shows the Elovich Model plot.

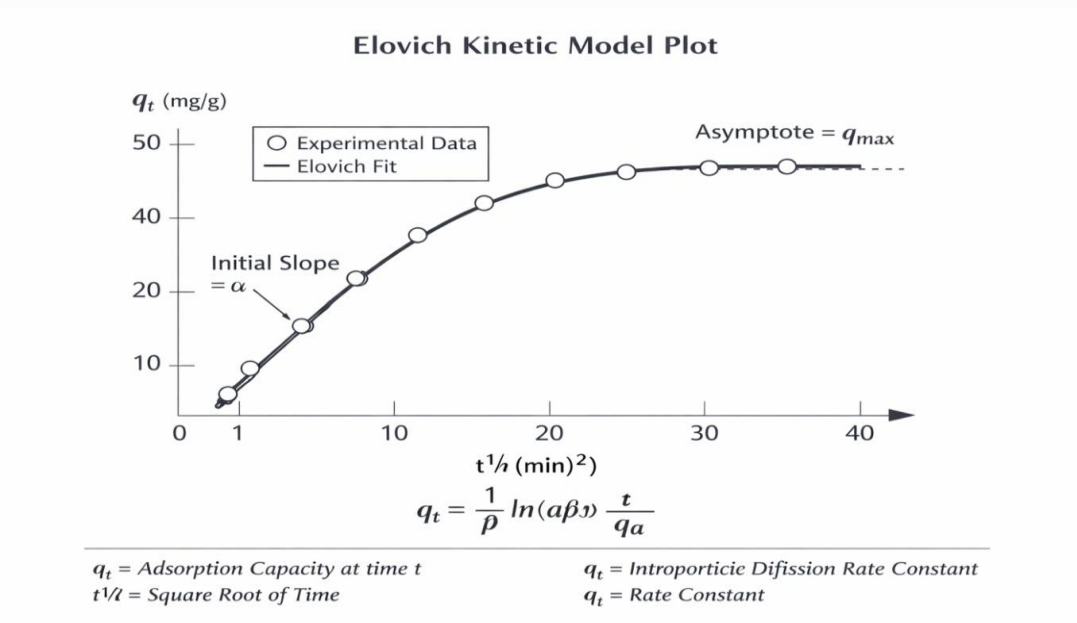

Figure 6. Elovich Model Plot

4.4 Intraparticle Diffusion Model

In most practical systems the overall rate is controlled not by surface binding alone but by sequential mass-transport steps: bulk diffusion through the fluid phase, diffusion across the stagnant film surrounding each particle, diffusion within the pore network, and finally adsorption at active sites. The Weber–Morris intraparticle-diffusion model is the standard tool for identifying whether pore diffusion contributes to rate limitation:

$$q_t = k_{id} t^{0.5} + C \quad (9)$$

Where:

k_{id}= Intraparticle diffusion rate constant (mg/g $min^{0.5}$),

C = Intercept, representing the boundary layer effect

A plot of q_t versus $t^{0.5}$ provides k_{id} as the slope and C as the intercept. If the plot is linear and passes through the origin ($C = 0$), intraparticle diffusion is the sole rate-limiting step. If it deviates, other processes such as film diffusion or surface adsorption are also involved.

Most real datasets produce multi-segment plots; an initial steep region reflecting rapid external transport, an intermediate linear region dominated by pore diffusion, and a final plateau approaching equilibrium. Relying exclusively on reaction-based models and ignoring transport steps is a major source of mechanistic misinterpretation in adsorption studies (Chu et al., 2025; Suneetha et al., 2015; H. Zhang et al., 2022). Figure 7 shows a depiction of the Intraparticle Diffusion (Weber-Morris) Plot.

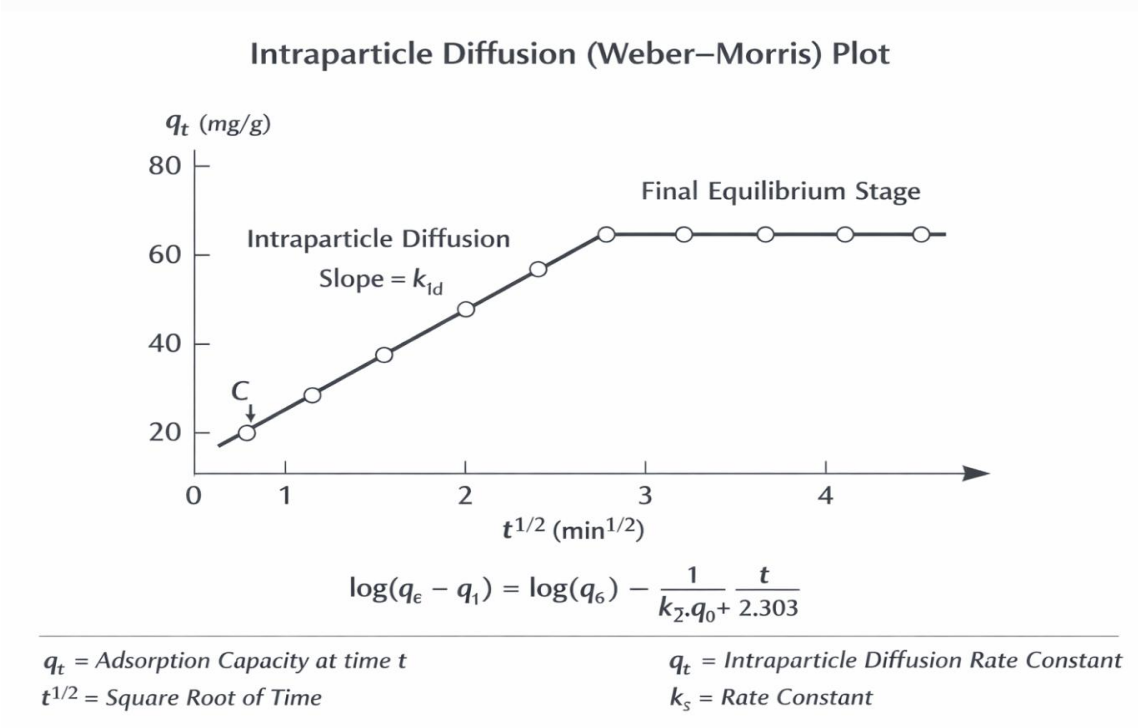

Figure 7. Intraparticle Diffusion (Weber-Morris) Plot

5. Experimental Design and Data Analysis

5.1 Data Collection Requirements

Robust kinetic data depend on careful experimental design:

1) **Sampling frequency:** collect points at short intervals (every 1–5 minutes) during the first 30–60 minutes, when uptake is fastest, extending intervals gradually as equilibrium is approached, sparse early sampling systematically distorts calculated rate constants;
2) **Controlled conditions:** maintain constant temperature, pH, agitation speed, adsorbent dosage, and initial adsorbate concentration across all runs;
3) **Replication:** perform all experiments in at least triplicate, and report mean values with standard deviation or confidence intervals;
4) **Blanks and controls:** include blank runs without adsorbent to account for adsorbate loss by wall adsorption, volatilisation, or precipitation.

5.2 Model Selection and Evaluation

Statistical goodness-of-fit alone is insufficient to select the "best" model, and the coefficient of determination is a particularly weak discriminator when computed on linearized transforms. Modern practice requires comparison using multiple criteria, computed wherever possible from nonlinear fits to the untransformed data:

1) Coefficient of determination (R^2) and adjusted R^2;
2) Standard error of the estimate;
3) Residual sum of squares (RSS):

$$RSS = \sum_{i=1}^{n}\left(q_{e,exp} - q_{e,cal}\right)^2 \quad (10)$$

4) Chi-squared statistic (χ^2):

$$(\chi^2) = \sum_{i=1}^{n}\frac{\left(q_{e,exp}-q_{e,cal}\right)^2}{q_{e,cal}} \quad (11)$$

the percentage deviation between experimental and calculated equilibrium uptake. It is important to avoid over-interpreting model preference: a model that fits marginally better mathematically does not necessarily reflect the actual physical process. All mechanistic claims must be supported by independent experimental evidence, not curve-fitting alone.

1. Comparative Summary Tables

Table 1: Comparative Analysis of Adsorption Kinetic Models

Model	Mathematical Form (Linearized)	Core Physical Assumptions	Primary Limitations	Best Practice Application
Pseudo-First-Order (Lagergren)	$\log(q_e - q_t) = \log q_e - \frac{k_1}{2.303}t$	Rate proportional to unoccupied site availability;	Fails past initial 20–30% uptake; systematically	Initial kinetic rate assessment;

		reversible process; no diffusion resistance.	underpredicts equilibrium capacity.	limited to early-stage rapid uptake.
Pseudo-Second-Order (Ho-McKay)	$\frac{t}{q_t} = \frac{1}{k_2 q_e^2} + \frac{1}{q_e} t$	Rate-limiting chemisorption step; rate proportional to square of available active sites.	High R^2 values are mathematically predisposed by linearization; does not prove chemisorption exclusively.	Broad evaluation across systems, provided non-linear regression is used for parameter extraction.
Elovich Model	$q_t = \frac{1}{\beta}\ln(\alpha\beta) + \frac{1}{\beta}\ln t$	Heterogeneous surface energy; activation energy increases linearly with surface coverage.	Inapplicable to pure physisorption on uniform, non-porous surfaces.	Characterizing complex materials (biochars, activated carbons, layered clays) with broad site energy distributions.
Intraparticle Diffusion (Weber-Morris)	$q_t = k_{id} t^{0.5} + C$	Pore diffusion is the sole rate-limiting mechanism when plots are linear and pass through the origin.	Often yields multi-segment plots where boundary-layer effects complicate direct interpretation.	Identifying mass-transport regimes and distinguishing external film diffusion from internal pore diffusion.

Table 2: Comparison of BET Analysis Parameters and Diagnostic Indicators

Diagnostic Parameter / Metric	Standard Range / Condition	Physical Meaning	Consequences of Violation / Misinterpretation
Relative Pressure Range (P/P_0)	$0.05 - 0.35$ (Default for non/mesoporous); lower for microporous	Valid region where multilayer physisorption dominates without micropore filling or capillary condensation.	Selecting points outside the range can introduce $> 30\%$ error in calculated surface area.
BET Constant (C)	$20 \leq C \leq 150$	Exponentially related to the difference between first-layer adsorption enthalpy and liquefaction enthalpy.	Negative intercepts invalidate the model; $C > 200$ indicates dominant micropore filling requiring alternative models (DR, t-plot).
Linear Regression (R^2)	≥ 0.995 (minimum), ≥ 0.999 (high-confidence)	Statistical measure of linear conformance within the selected relative pressure interval.	Arbitrarily adjusting pressure windows solely to inflate R^2 yields mathematically optimized yet physically invalid surface areas.

Critical Synthesis, Unresolved Issues, and Recommendations in Adsorption Characterization

It is clear from the literature that there has always been a conflict between the two empirical convenience and rigorous physical chemistry in characterization of porous materials. Variations in pretreatment protocols, and arbitrary relative-pressure windows, result in significant differences in the surface area reported in landmark interlaboratory studies, which show that the Brunauer–Emmett–Teller equation cannot be used as a black-box model of surface area, and that it fails to capture important factors such as surface heterogeneity. Likewise, in turn historical kinetic models are plagued by the use of linear regression, which is not critical and leads to non-realistic error structures and correlation coefficients. This underscores the methodological gap in characterizing locally-sourced bio-adsorbents since their preparation varies for each location, making them incomparable globally.

The challenges are rooted in four issues that have not yet been resolved: first, there is no consistency in the selection of pressure points that are reported; second, there is the potential for 'mathematical goodness of fit' to be confused with 'true physical mechanisms'; third, there are deficiencies of reproducibility due to the fact that the complex bio-derived structures are evaluated without an accompanying profile; and fourth, there are common omissions of operational metadata. These inadequacies need to be addressed with the application of scientific norms and scientific rigour. Recommendations for researchers include employing non-linear regression for parameter extraction, objective range-selection criteria over fixed pressure windows, multi-technique validation tools such as Fourier-transform infrared spectroscopy and pore-size distribution kernel, and promotion of the use of FAIR data principles through the use of existing Adsorption Information File repositories. Adopting these technical standards ensures methodological consistency in various scientific applications, improves professional skills, integrity of data, and sustainable use of resources (Onyiorah, 2025; Ofozoba et al., 2025; Emeasoba et al., 2026; Aguma et al., 2026; Alegbeleye et al., 2025; Ibeh & Akinyele, 2024)

Conclusion

BET gas adsorption and kinetic modelling remain indispensable tools for porous-materials research, but their scientific value depends entirely on rigorous implementation and thoughtful interpretation. Interlaboratory studies and the current IUPAC recommendations have shown that deviations from standardized, criterion-based procedures; whether in sample preparation, pressure-range selection, fitting method, or reporting practice can introduce discrepancies

exceeding 30 % in calculated surface area and lead to flawed mechanistic conclusions from kinetic data.

For BET analysis, objective range selection via the Rouquerol criteria, appropriate choice of probe gas (argon at 87 K for micropore analysis; krypton at 77 K for low-area samples), and transparent reporting of all experimental parameters are essential (F. Rouquerol et al., 1999). Kinetic studies should fit untransformed models by nonlinear regression, test multiple models, use complementary statistical metrics, and avoid equating mathematical fit with proof of mechanism. Wherever possible, findings should be corroborated by independent characterization of pore structure and surface chemistry.

For emerging research areas, including locally sourced bio-adsorbents, nanostructured catalysts, and hierarchical porous materials, greater emphasis on interlaboratory calibration and open data sharing will be critical to improving comparability and accelerating progress. Future advances are likely to combine traditional adsorption measurements with in-situ imaging, computational modelling, and machine learning to develop more accurate, mechanism-aware characterization frameworks that better link material structure to functional performance

References

Aguma, Q., Nanjundaswamy, A., Omolewa, J. O., Choko, O. P., Onakpoma, I., Ibeh, K. G., & Okon, K. E. (2026). Bioactive Terpenoids from Desert Shrubs for Durable Wood Protection: Chemistry, Delivery Systems, and Circular Bioresource Integration. *BioResources*, *21*(1), 2710-2757. https://ojs.bioresources.com/index.php/BRJ/article/view/25300

Alegbeleye, O. M., Meddens, A. J. H., Rotimi, Y. O., & Ibeh, K. G. (2025). Urban tree crown detection based on deep learning and high-resolution aerial imagery: PTCNet for Pullman, WA, USA. *Remote Sensing Applications: Society and Environment*, 101818. https://doi.org/10.1016/j.rsase.2025.101818

Al Rammah, A. F., Rajagopalan, A. K., Sarkisov, L., & Siperstein, F. R. (2025). Understanding errors in gas adsorption at low pressures: the case of direct air capture. *Adsorption 2025 31:6*, *31*(6), 94-. https://doi.org/10.1007/S10450-025-00644-1

Bourafa, A., Berrich, E., Belhachemi, M., Jellali, S., & Jeguirim, M. (2024). Preparation and characterization of hydrochars and CO2-activated hydrochars from date and olive stones. *Biomass Conversion and Biorefinery*, *14*(17), 20385–20396. https://doi.org/10.1007/S13399-023-04225-6

Brunauer, S., Emmett, P. H., & Teller, E. (1938). Adsorption of gases in multimolecular layers. *J Am Chem Soc*, *60*(2), 309–319. https://doi.org/10.1021/ja01269a023

Chin, J. F., Heng, Z. W., Teoh, H. C., Chong, W. C., & Pang, Y. L. (2022). Recent development of magnetic biochar crosslinked chitosan on heavy metal removal from wastewater – Modification, application and mechanism. *Chemosphere*, *291*. https://doi.org/10.1016/J.CHEMOSPHERE.2021.133035

Chrouda, A., Briki, C., Slimi, K., Jemni, A., & Ahmadipour, M. (2025). Synthesis of highly porous covalent organic frameworks for green hydrogen storage applications. *Journal of the Taiwan Institute of Chemical Engineers*, *170*. https://doi.org/10.1016/j.jtice.2025.106005

Chu, K. H., Hashim, M. A., Zawawi, M. H., & Bollinger, J. C. (2025). The Weber–Morris model in water contaminant adsorption: Shattering long-standing misconceptions. *Journal of Environmental Chemical Engineering*, *13*(4), 117266. https://doi.org/10.1016/J.JECE.2025.117266

Chun, D. D., Ni, D., & Simson, A. (2022). The effect of inherent inorganics and CO2 co-pyrolysis on biochar production from biowastes and their gasification reactivity. *Biomass and Bioenergy*, *158*. https://doi.org/10.1016/j.biombioe.2022.106361

Emeasoba, N.C., Onyiorah, B.O., Eneogwe, V.N., VictorIgwe, J.N., Akpa, C.C., Adieze, C., Akudolu, C.A., Nwatarali, C.N., Ndom-Uchendu, M.N., Ikpeama, F.U. and Paul-Mgbeafulike, V.S., 2026. Influence of debt and risk management skills on the management of small and medium scale enterprises (SMES) in Umuahia Metropolis, Abia State, Nigeria. *Veredas do Direito*, *23*(8), pp.e236253-e236253. https://doi.org/10.48047/gg2rpy35

Ezenwa, O. N., Mgbemena, C. O., & Emagbetere, E. (2024). Utilization of solid residue from hydrothermal liquefaction of breadfruit pulp for the production of bio-briquette using cassava starch as binder. *Heliyon*, *10*(1), e24081. https://doi.org/10.1016/j.heliyon.2024.e24081

Francis, J. C., Nighojkar, A., & Kandasubramanian, B. (2023). Relevance of wood biochar on CO2 adsorption: A review. *Hybrid Adv*, *3*, 100056. https://doi.org/10.1016/j.hybadv.2023.100056

Galarneau, A., Mehlhorn, D., Guenneau, F., Coasne, B., Villemot, F., Minoux, D., Aquino, C., & Dath, J. P. (2018). Specific Surface Area Determination for Microporous/Mesoporous Materials: The Case of Mesoporous FAU-Y Zeolites. *Langmuir*, *34*(47), 14134–14142. https://doi.org/10.1021/acs.langmuir.8b02144

Ganguly, P., Sarkhel, R., & Das, P. (2020). Synthesis of pyrolyzed biochar and its application for dye removal: Batch, kinetic and isotherm with linear and non-

linear mathematical analysis. *Surfaces and Interfaces*, *20*. https://doi.org/10.1016/J.SURFIN.2020.100616

Goel, C., Mohan, S., & Dinesha, P. (2021). CO2 capture by adsorption on biomass-derived activated char: A review. *Sci Total Environ*, *798*, 149296. https://doi.org/10.1016/j.scitotenv.2021.149296

Hameed, B. H., & Ahmad, A. A. (2009). Batch adsorption of methylene blue from aqueous solution by garlic peel, an agricultural waste biomass. *Journal of Hazardous Materials*, *164*(2–3), 870–875. https://doi.org/10.1016/j.jhazmat.2008.08.084

Ho, Y. S., & McKay, G. (1999). Pseudo-second order model for sorption processes. *Process Biochemistry*, *34*(5), 451–465. https://doi.org/10.1016/S0032-9592(98)00112-5

Intriago, D., Raman, A. S., & Vojvodic, A. (2026). On the Predictability and Fundamental Insights of Adsorption Models: Current Status and the Path Ahead. *ChemPhysChem*, *27*(12), e70436. https://doi.org/10.1002/CPHC.70436;WGROUP:STRING:PUBLICATION

Ibeh, K. G., & Akinyele, A. O. (2024). Investigating Light and Water Optimization for Early Seedling Establishment in Albizia lebbeck (L.) Benth. *South-east European forestry: SEEFOR*, *15*(2), 151-159. https://doi.org/10.15177/seefor.24-14

ISO. (2022). *Determination of the specific surface area of solids by gas adsorption — BET method* (Vol. 2022).

Jiang, Y., Li, T., Xu, X., Sun, J., Pan, G., & Cheng, K. (2024). A global assessment of the long-term effects of biochar application on crop yield. *Current Research in Environmental Sustainability*, *7*. https://doi.org/10.1016/J.CRSUST.2024.100247

Lagergren, S. (1898). About the Theory of So-Called Adsorption of Soluble Substances. *Kungliga Svenska Vetenskapsakademiens*, *24*(4), 1–39. https://sid.ir/paper/563615/en

Langmuir, I. (1917). The constitution and fundamental properties of solids and liquids. *Journal of the Franklin Institute*, *183*(1), 102–105. https://doi.org/10.1016/S0016-0032(17)90938-X

Liu, C., Fu, C., Li, T., Zhang, P., Xia, Y., Wu, Y., Lan, Q., Li, Y., Zhang, Y., & Gui, J. (2023). CO2 capture using biochar derived from conditioned sludge via pyrolysis. *Sep Purif Technol*, *314*, 123624. https://doi.org/10.1016/j.seppur.2023.123624

Liu, T., Lawluvy, Y., Shi, Y., Ighalo, J. O., He, Y., Zhang, Y., & Yap, P. S. (2022). Adsorption of cadmium and lead from aqueous solution using modified

biochar: A review. *Journal of Environmental Chemical Engineering*, *10*(1). https://doi.org/10.1016/j.jece.2021.106502

Mgbemena, C. O., Ibekwe, N. O., Sukumar, R., & Menon, A. R. R. (2013). Characterization of kaolin intercalates of oleochemicals derived from rubber seed (Hevea brasiliensis) and tea seed (Camelia sinensis) oils. *Journal of King Saud University - Science*, *25*(2), 149–155. https://doi.org/10.1016/j.jksus.2012.11.004

Ndukwu, M. C., Ehiem, J., Mbanasor, J., & Obasi, N. (2022). Thermal softening kinetics of African black olive fruit: Influence of temperature and water absorption on the thermal maceration dynamics and thermophysical properties. *Journal of Food Processing and Preservation*, *46*(11). https://doi.org/10.1111/JFPP.17021

Odeh, C. P., Mgbemena, C. O., Oreko, B. U., & Mgbemena, C. E. (2025). Impact of processing parameters on the hydrothermal carbonisation of African Elemi Shell. *Journal of Umm Al-Qura University for Engineering and Architecture*. https://doi.org/10.1007/S43995-025-00135-Y

Offiah, V. O., & Falade, K. O. (2023). Potentials of baobab in food systems. *Applied Food Research*, *3*(1), 100299. https://doi.org/10.1016/J.AFRES.2023.100299

Ofozoba, C.A., Okafor, P.C., Ikegbusi, N.G., Manafa, F.U., Egwu, J.U., Nwobu, C.M., Okafor, S.O., Onafowope, M.A., Olofinkua, V.K., Adeagbo, J.O. and Gbaeprekumo, O.V., 2025. AI-driven service-learning to enhance students' understanding of green nanomaterials in sustainability education. *Multidisciplinary Reviews*, *8*(12), p.2025429. https://10.31893/multirev.2025429

Onyiorah, B. O. (2025). Artificial intelligence skill development as a predictor of job readiness among business education undergraduates in tertiary institutions in Anambra State, Nigeria. *Journal of Investment Development, Economics and Accounting*, *2*(2), 114-126. https://doi.org/10.70001/jidea.v2i2.406

Osterrieth, J. W. M., Rampersad, J., Madden, D., Rampal, N., Skoric, L., Connolly, B., Allendorf, M. D., Stavila, V., Snider, J. L., Ameloot, R., Marreiros, J., Ania, C., Azevedo, D., Vilarrasa-Garcia, E., Santos, B. F., Bu, X. H., Chang, Z., Bunzen, H., Champness, N. R., … Fairen-Jimenez, D. (2022). How Reproducible are Surface Areas Calculated from the BET Equation? *Advanced Materials*, *34*(27), 2201502. https://doi.org/10.1002/adma.202201502

Pap, S., Shearer, L., & Gibb, S. W. (2025). Sustainable remediation of macrolide antibiotic from water using a novel Fe oxide/biochar nanocomposite: Adsorption behaviour and mechanistic analysis. *Journal of Environmental Chemical Engineering*, *13*(1). https://doi.org/10.1016/j.jece.2024.115208

Ramezanipour Penchah, H., Ghaemi, A., & Jafari, F. (2022). Piperazine-modified activated carbon as a novel adsorbent for CO2 capture: modeling and characterization. *Environmental Science and Pollution Research*, *29*(4), 5134–5143. https://doi.org/10.1007/S11356-021-16040-5

Revellame, E. D., Fortela, D. L., Sharp, W., Hernandez, R., & Zappi, M. E. (2020). Adsorption kinetic modeling using pseudo-first order and pseudo-second order rate laws: A review. *Cleaner Engineering and Technology*, *1*. https://doi.org/10.1016/j.clet.2020.100032

Rouquerol, F., Jean, R., & Sing, K. (1999). *Chapter 3 - methodology of adsorption at the gas–solid interface* (pp. 51–92). Academic Press.

Rouquerol, J., Llewellyn, P., & Rouquerol, F. (2007). Is the BET equation applicable to microporous adsorbents? *Studies in Surface Science and Catalysis*, *160*, 49–56. https://doi.org/10.1016/S0167-2991(07)80008-5

Suneetha, M., Sundar, B. S., & Ravindhranath, K. (2015). Removal of fluoride from polluted waters using active carbon derived from barks of Vitex negundo plant. *Journal of Analytical Science and Technology*, *6*(1). https://doi.org/10.1186/S40543-014-0042-1

Thommes, M., Kaneko, K., Neimark, A. V., Olivier, J. P., Rodriguez-Reinoso, F., Rouquerol, J., & Sing, K. S. W. (2015). Physisorption of gases, with special reference to the evaluation of surface area and pore size distribution (IUPAC Technical Report). *Pure and Applied Chemistry*, *87*(9–10), 1051–1069. https://doi.org/10.1515/PAC-2014-1117

Tong, D. S., Wu, C. W., Adebajo, M. O., Jin, G. C., Yu, W. H., Ji, S. F., & Zhou, C. H. (2018). Adsorption of methylene blue from aqueous solution onto porous cellulose-derived carbon/montmorillonite nanocomposites. *Applied Clay Science*, *161*, 256–264. https://doi.org/10.1016/J.CLAY.2018.02.017

Vareda, J. P. (2023). On validity, physical meaning, mechanism insights and regression of adsorption kinetic models. *Journal of Molecular Liquids*, *376*. https://doi.org/10.1016/j.molliq.2023.121416

Vashishtha, M., & Kumar, K. V. (2026). Insights into Solid–Liquid Adsorption Kinetics: Theory, Mechanisms, and Practical Guidelines. *ACS ES&T Water*, *6*(5), 2569–2601. https://doi.org/10.1021/ACSESTWATER.5C00497

Wang, T., Liu, F., Ge, K., & Fang, M. (2017). Reaction kinetics of carbon dioxide absorption in aqueous solutions of piperazine, N-(2-aminoethyl) ethanolamine and their blends. *Chemical Engineering Journal*, *314*, 123–131. https://doi.org/10.1016/j.cej.2016.12.129

Xia, X., Jiao, X., Li, J., Shen, W., Xia, Y., & Wang, H. (2024). Gas adsorption behavior in shale reservoirs: Insights from molecular scale. *Capillarity*, *13*(3), 68–72. https://doi.org/10.46690/CAPI.2024.12.03

Yazidi, I., Ziat, K., Bardiji, N. El, Boundati, Y. El, Naji, A., Haskouri, J. El, & Saidi, M. (2026). *Adsorption Kinetics, Isotherm Models, and Thermodynamics: A Brief Review BT - Artificial Intelligence and Emerging Materials for the Transition Toward Green and Smart Technologies*. 93–105. https://doi.org/10.1007/978-3-032-15481-1_8

Yek, P. N. Y., Peng, W., Wong, C. C., Liew, R. K., Ho, Y. L., Wan Mahari, W. A., Azwar, E., Yuan, T. Q., Tabatabaei, M., Aghbashlo, M., Sonne, C., & Lam, S. S. (2020). Engineered biochar via microwave CO2 and steam pyrolysis to treat carcinogenic Congo red dye. *Journal of Hazardous Materials*, *395*. https://doi.org/10.1016/J.JHAZMAT.2020.122636

Zhang, H., Tian, S., Zhu, Y., Zhong, W., Qiu, R., & Han, L. (2022). Insight into the adsorption isotherms and kinetics of Pb (II) on pellet biochar via in-situ non-destructive 3D visualization using micro-computed tomography. *Bioresource Technology*, *358*. https://doi.org/10.1016/J.BIORTECH.2022.127406

Zhang, K., & Zhang, H. (2025). Data-Centric Approach for Modeling the Adsorption of Small Gas Molecules on Granular Activated Carbons. *Environmental Science and Technology*, *59*(22), 11063–11072. https://doi.org/10.1021/ACS.EST.4C12168